RESEARCH ARTICLE

Essential tremor severity and anatomical changes in brain areas controlling movement sequencing

Julián Benito-León[1,2,3], José Ignacio Serrano[4], Elan D. Louis[5,6,7], Ales Holobar[8], Juan P. Romero[9,10], Petra Povalej-Bržan[8,11], Jernej Kranjec[8], Félix Bermejo-Pareja[2,3,12], María Dolores del Castillo[4], Ignacio Javier Posada[1,3] & Eduardo Rocon[4]

[1]Department of Neurology, University Hospital, 12 de Octubre, Madrid, Spain
[2]Center of Biomedical Network Research on Neurodegenerative Diseases (CIBERNED), Madrid, Spain
[3]Department of Medicine, Faculty of Medicine, Complutense University, Madrid, Spain
[4]Neural and Cognitive Engineering group, Centre for Automation and Robotics (CAR) CSIC-UPM, Arganda del Rey, Spain
[5]Department of Neurology, Yale School of Medicine, New Haven, Connecticut
[6]Department of Chronic Disease Epidemiology, Yale School of Public Health, New Haven, Connecticut
[7]Center for Neuroepidemiology and Clinical Neurological Research, Yale School of Medicine and Yale School of Public Health, New Haven, Connecticut
[8]Faculty of Electrical Engineering and Computer Science, University of Maribor, Maribor, Slovenia
[9]Faculty of Biosanitary Sciences, Francisco de Vitoria University, Pozuelo de Alarcón, Madrid, Spain
[10]Brain Damage Service, Hospital Beata Maria Ana, Madrid, Spain
[11]Faculty of Health Sciences, University of Maribor, Maribor, Slovenia
[12]Clinical Research Unit, University Hospital, 12 de Octubre, Madrid, Spain

Correspondence
Julián Benito-León, Av. de la Constitución 73, portal 3, 7° Izquierda, 28821 Coslada, Madrid, Spain. Tel: +34916695467; E-mail: jbenitol67@gmail.com

Abstract

Objective: Although the cerebello-thalamo-cortical network has often been suggested to be of importance in the pathogenesis of essential tremor (ET), the origins of tremorgenic activity in this disease are not fully understood. We used a combination of cortical thickness imaging and neurophysiological studies to analyze whether the severity of tremor was associated with anatomical changes in the brain in ET patients. **Methods**: Magnetic resonance imaging (MRI) and a neurophysiological assessment were performed in 13 nondemented ET patients. High field structural brain MRI images acquired in a 3T scanner and analyses of cortical thickness and surface were carried out. Cortical reconstruction and volumetric segmentation was performed with the FreeSurfer image analysis software. We used high-density surface electromyography (hdEMG) and inertial measurement units (IMUs) to quantify the tremor severity in upper extrimities of patients. In particular, advanced computer tool was used to reliably identify discharge patterns of individual motor units from surface hdEMG and quantify motor unit synchronization. **Results**: We found significant association between increased motor unit synchronization (i.e., more severe tremor) and cortical changes (i.e., atrophy) in widespread cerebral cortical areas, including the left medial orbitofrontal cortex, left isthmus of the cingulate gyrus, right paracentral lobule, right lingual gyrus, as well as reduced left supramarginal gyrus (inferior parietal cortex), right isthmus of the cingulate gyrus, left thalamus, and left amygdala volumes. **Interpretation**: Given that most of these brain areas are involved in controlling movement sequencing, ET tremor could be the result of an involuntary activation of a program of motor behavior used in the genesis of voluntary repetitive movements.

Introduction

Essential tremor (ET) is a neurodegenerative disorder with a wide clinical spectrum, including several motor and non-motor features.[1] Although the cerebello-thalamo-cortical network has often been suggested to be of importance in the pathogenesis of ET, the origins of tremorgenic activity in this disease are not fully understood. Through analyses of coherence between cerebral cortical and muscle activity, several studies have demonstrated the presence of tremor-related activity in cerebral cortical structures;[2,3] however, these findings have not been replicated by others.[4] These discrepancies could be the result of intermittent cortico-muscular coupling. In fact, it has been suggested that this "cortico-muscular coupling" might be affected by bilateral motor synchronization and awareness of tremor.[4] In line with this, a recent study using functional magnetic resonance imaging (MRI) has revealed that increases in visual feedback exacerbate the severity of tremor in ET patients.[5] Furthermore, the latter study has also suggested the presence of a widespread functional network across cerebellum, motor cortex, extra-striate visual cortex, and parietal cortex associated with tremor severity in ET patients.[5] However, to our knowledge, the relationship between structural cortico-metric changes and the severity of ET tremor has not been explored and elucidated. The identification of brain structural abnormalities associated with the severity of tremor would add to the available evidence concerning the role of the cortex in the genesis and/or propagation of tremor in ET.

Only three studies have assessed the pattern of cortical thickness in ET.[6–8] Chung et al.[6] studied the pattern of cortical thickness in 18 ET patients who had responded to propranolol and 14 who had not. The non-responder group had more severe thinning in the left orbitofrontal cortex and right temporal cortex.[6] In a voxel-based morphometry and cortical thickness study involving 14 ET patients, 12 dystonia patients, and 23 age- and sex-matched healthy control subjects, Cerasa et al.[7] reported subtle thinning of the anterior cerebellar cortex in the ET patients. Serrano et al.,[8] tested the informativeness of measuring cortical thickness for the purposes of ET diagnosis, applying feature selection and machine learning methods to study a sample of 18 patients with ET and 18 age- and sex-matched healthy control subjects. They found that cortical thickness features alone distinguished the two, ET from healthy controls, with 81% diagnostic accuracy.[8]

Our main aim was to objectify how the anatomical integrity of brain structures in ET might be related to tremorgenic activity. Given the relationship between Parkinson's disease and ET,[9] we hypothesized that the anatomical integrity of several specific brain areas might be associated with tremorgenic activity in ET (esp., frontal and parietal areas involved in movement sequencing), similar to that suggested for Parkinson's disease.[10] Toward this purpose, we used a combination of cerebral cortical thickness imaging and neurophysiological studies (high-density electromyography [hdEMG] and inertial measurement units [IMUs]) to analyze whether the severity of tremor in ET, measured by the level of motor unit synchronization,[8,11] was associated with the integrity of brain anatomical structures. A secondary aim was to compare the brain anatomical structure of the ET group with that of a healthy control group.

Methods

Ethical aspects

All the participants included in the study gave their written informed consent after full explanation of the

procedure. The study, which was conducted in accordance with the principles of the Helsinki declaration of 1975, was approved by the ethical standards committee on human experimentation at the University Hospital "12 de Octubre" (Madrid).

Participants

ET patients were consecutively recruited from October 2012 to July 2013 from the outpatient neurology clinics of the University Hospital "12 de Octubre" in Madrid (Spain) after obtaining an appropriate informed consent. Patients with history of dementia, stroke, epilepsy, head injury or serious medical illness were excluded. We collected data on demographics and medications to exclude patients with tremor from hyperthyroidism or other medical conditions or medication-induced tremor. Clinical characteristics were obtained from review of records from their outpatient neurological care. Furthermore, based on a detailed clinical mental status examination, we excluded patients with Diagnostic and Statistical Manual of Mental Disorders (DSM)–IV criteria for dementia.[12]

Two neurologists with expertise in movement disorders (JB-L and JPR), who were blinded to the MRI results, examined the patients and used the Fahn-Tolosa-Marín tremor rating scale to assign a total tremor score (range = 0–144).[13] Diagnoses of ET were assigned by two neurologists (JB-L and JPR) using the Consensus Statement on Tremor by the Movement Disorder Society.[14] Furthermore, all ET patients had a normal [(123) I]FP-CIT single photon emission computed tomography scan.

Seventeen age, gender, and education-matched healthy controls were recruited either from relatives or friends of the health professionals working at the University Hospital "12 de Octubre" of Madrid (Spain) or among the relatives of patients who came to the neurological clinics for reasons other than ET (e.g., headache, dizziness). None reported having a first-degree or second-degree relative with ET. Each control was examined by two neurologists (JB-L and JPR), who were blinded to the MRI results, to further rule out any neurological or other serious conditions, including movement disorders, dementia, stroke, epilepsy, or head injury.

All of the neurophysiological and MRI studies (see below) were performed during the same week and while taking their regular daily medication for ET. Detailed accounts of the neurophysiological and neuroimaging procedures have been published previously.[8,10,15]

Neurophysiological procedures

Every recording was carried out in a dimly illuminated room. Patients seated in a comfortable armchair were instructed to relax and keep their gaze fixed on a wall at ~2-m distance. Postural and rest tremor were stimulated by the tasks described in Table 1. In order to enhance their tremor, patients with mild tremor severity were additionally asked to mentally count backward during the recordings. The recordings ranged from 40 sec to 4 min in duration, where at the 30 sec long interval with the maximum tremor amplitude was selected for the analysis.

Assessment of tremor in wrist movements

We used two pairs of IMUs (Technaid S.L., Madrid, Spain) to measure movements of left and right wrist. One IMU was placed on the dorsum of the hand and the other on the distal third of the forearm. The IMUs signals were sampled at 100 Hz and 12-bit resolution, low pass filtered (cutoff frequency of 20 Hz) and stored for off-line processing.

The coordinate systems of both IMUs in each pair had *y*-axis aligned and the differences between the accelerations in this axis were used to quantify the wrist movements. In particular, Welch's power spectral density (PSD) was calculated in MATLAB (The MathWorks, Natick, MA) using the 1 sec long signal segments.

The tremor frequency was defined as the frequency of maximum PSD peak on the interval from 5 Hz to 12 Hz. Tremor harmonics were identified as the frequencies of local PSD peaks at the double, triple and quadruple tremor frequency with tolerance of ± 0.5 Hz. The amplitudes of detected PSD peaks at tremor frequency and its harmonics were then expressed in logarithmic scale and averaged, yielding the mean logarithmic tremor power, that

Table 1. Tremor-triggering tasks performed during recordings of wrist movement and hdEMG metrics. Each task was performed three times.

Task	Description
Rest (RE)	The patient rested both arms, which were completely relaxed and supported either on the armrests or on the patient's lap, depending on what he/she reported to be most comfortable
Arms outstretched (AO)	The patient kept his/her arms outstretched, parallel to the ground, with the palms down and the fingers apart
Arms outstretched with weights (WE)	The same as the AO task but with one-kilogram weight fixed to both hands
Arms supported + postural tremor elicited (PO)	The same as RE task, but with hands and fingers extended against gravity

is, tremor severity. With this approach we increased the relative contributions of small PSD peaks and stressed the role of higher tremor harmonics.

The rational for this nonlinear weighting of the PSD peaks is based on the hypothesis that both the level of muscle excitation and the level of motor unit synchronization contribute to the tremor severity.[11,15–17] That is to say, in pathological tremor, synchronization of motor unit activity in muscles causes involuntary bursts of muscle activity and these bursts result in wrist oscillations.[11,17] The stronger the pathological muscle excitation (i.e., the larger the number of activated motor units), the stronger the amplitude of wrist oscillations and the stronger the power of basic tremor frequency.[11,17] Similarly, the stronger the synchronization of motor unit spike trains, the higher the regularity of tremor bursts and the larger the higher harmonics in the neural drive to the muscle and also in the inertial measurements of wrist oscillation.[16]

The sum of individual motor unit spike trains, the so called cumulative spike train (CST), correlates linearly with the neural drive to the muscle.[18] The higher the level of motor unit synchronization, the steeper the rises (at the start of the tremor burst) and falls (at the end of the tremor burst) in the CST.[18–20] Therefore, with increase in motor unit synchronization, the CST becomes more and more similar to the periodic rectangular signal.[18] In the extreme case of perfect motor unit synchronization, the CST becomes a delta train,[18] and its Fourier transform is a delta train with frequency peaks at higher harmonics of basic tremor frequency.[21] Similarly, Fourier transform of a periodic rectangular signal contains many higher harmonics of basic tremor frequency.[22] Hence, the amplitude and the number of higher harmonics in the neural drive, EMG or inertial measurements depend on the steepness of the rising and falling edges in CST and, thus, on the level of motor unit synchronization.

Noteworthy, mechanical properties of wrist low-pass filter the muscle excitation patterns in the mechanical tremor signals (e.g., force or acceleration) and suppress the relative contributions of higher tremor harmonics.[15] Therefore, logarithmic weighting of PSD peaks was used in the current study to counteract this low-pass filtering effect and to increase the weight of tremor regularity in the estimated tremor severity. The use of logarithmic function was motivated by other studies reported in the literature.[23,24]

Mean logarithmic tremor power was averaged over all the postural tasks (arms outstretched [AO], arms supported + postural tremor elicited [PO] and arms outstretched with weights [WE]) and the rest (RE) task (Table 1). The following tremor features were extracted from the IMUs recordings.[15]

- Mean logarithmic power of the tremor harmonics, averaged over the AO, PO, WE and RE tasks in both hands. This metric reflects the net effect of all the muscles that affect the wrist movement. Generally speaking, the higher the metric's value, the higher the synchronization of motor unit activity in muscles controlling the wrist.
- Mean logarithmic power of the tremor harmonics, averaged over the AO, PO, and WE tasks, and normalized to RE task in both hands. This metric quantifies how the synchronization of muscles and motor units changes when patients switch from RE to postural task. Positive values indicate stronger synchronization in postural task than in RE task, whereas negative values indicate the stronger synchronization in RE than in postural tasks.
- The difference between the mean logarithmic tremor power, averaged across all the postural tasks (AO, PO, WE), and the mean logarithmic tremor power, averaged across the RE task.

Despite all these metrics used, the level of muscle excitation and the level of motor unit synchronization are difficult to discriminate using IMUs. For this purpose, we directly measured motor unit synchronization by the means of hdEMG decomposition, as described below.

Surface hdEMG signals

Surface hdEMG signals were recorded with 5×13 electrode arrays (LISiN–OT Bioelettronica, Torino, Italy, 8 mm interelectrode distance) centred over flexor carpi radialis and extensor digitorum communis, respectively. Before electrode placement, we cleaned the skin and lightly abraded it with abrasive paste (Meditec–Every, Parma, Italy). In order to improve the electrode-skin contact, the electrode cavities in the array were filled with conductive gel (Meditec–Every, Parma, Italy). A soaked bracelet, placed around one of the wrists was used as a reference electrode. The bipolar surface hdEMG recordings were amplified, band-pass filtered (3 dB bandwidth, 10–750 Hz) and sampled at 2048 Hz and 12–bit resolution (LISiN–OT Bioelettronica, Torino, Italy).

We used Convolution Kernel Compensation (CKC) algorithm.[25,26] to independently decompose the hdEMG signals from each array into motor unit spike trains. CKC algorithm linearly combines all the channels from hdEMG array and estimates the firing times (i.e., spikes) of individual motor units. Afterwards, we used the Pulse-to-Noise Ratio (PNR) to assess the accuracy of each individual motor unit spike train estimation.[27] Only the motor units with PNR $\geq$ 30 dB (corresponding to accuracy in identification motor unit firing of >90%) were kept for

analysis, whereas all the remaining motor units were discarded. In addition, every identified motor unit spike train was manually inspected by two experienced operators and obvious errors in automatic decomposition corrected.

Finally, we quantified the pair-wise motor unit synchronization. For this purpose, we calculated backward and forward motor unit recurrence times in pairs of simultaneously active motor units.[28] The forward (backward) recurrence time was defined as the distance from the discharge of the first motor unit to the closest next (previous) discharge of the second motor unit.[29] For each pair of identified motor units, we computed the 99% confidence limit in a histogram of motor unit recurrence times, assuming their uniform distribution in the absence of pathological tremor.[29] We then defined the percentage of concurrent motor unit discharges as the ratio between the peak area exceeding this 99% limit and the total number of recurrence times in the histogram. Finally, we averaged the percentage of concurrent motor unit discharges across all the pairs of identified motor units per recorded muscle.

The percentage of concurrent motor unit discharges in postural tasks was normalized with the percentage of concurrent motor unit discharges during the RE task. Therefore, values greater than 1 indicate stronger motor unit synchronization in postural tasks than in RE task, whereas values lower than 1 indicate stronger motor unit synchronization in RE task than in postural tasks.

Neuroimaging procedures

Neuroimage acquisition

Participants were immobilized with a custom-fit blue bag vacuum mold (Medical Intelligence, Inc.) to prevent image artifacts. A strict criterion for head movement assessment was adopted (maximal absolute head movement less than 1.0 mm and 1.0° in the x, y, and z directions). Neither patients nor healthy controls were excluded from the analysis due to this criterion. MRI data were acquired on each patient and healthy control using a GE Signa 3.0 T scanner (General Electric Medical Systems, Milwaukee, WI) with a standard quadrature birdcage headcoil, using an axial 3D T1-weighted inversion-recovery fast gradient echo sequence (TR = 5.0 msec; TE = 2.2 msec; Flip Angle = 12°; TI = 750 msec; NEX = 1.0). A total of 176 contiguous 1-mm slices were acquired with a 240 × 240 matrix with an in-plane resolution of 1 × 1 mm, resulting in isotropic voxels. Standard sequences of the MRI scans were checked before inclusion of a patient or healthy control.

Neuroimage processing

MRI images were processed to extract two types of information: volumetric features and cortical thickness features. Cortical reconstruction and volumetric segmentation was performed with the FreeSurfer image analysis suite, which is documented and freely available for download online (http://surfer.nmr.mgh.harvard.edu/). Briefly, this processing includes motion correction and averaging[30] of multiple volumetric T1 weighted images (when more than one is available), removal of non-brain tissue using a hybrid watershed/surface deformation procedure,[31] automated Talairach transformation, segmentation of the subcortical white matter and deep gray matter volumetric structures (including hippocampus, amygdala, caudate, putamen, ventricles),[32] intensity normalization,[33] tessellation of the gray matter white matter boundary, automated topology correction,[34] and surface deformation following intensity gradients to optimally place the gray/white and gray/cerebrospinal fluid borders at the location where the greatest shift in intensity defines the transition to the other tissue class.[35] Once the cortical models were complete, a number of deformable procedures could be performed for further data processing and analysis; these included surface inflation,[36] registration to a spherical atlas, which utilizes individual cortical folding patterns to match cortical geometry across subjects,[37] fragmentation of the cerebral cortex into units based on gyral and sulcal structure,[38] and creation of a variety of surface-based data including maps of curvature and sulcal depth. This method used both intensity and continuity information from the entire three dimensional MRI volume in segmentation and deformation procedures to produce representations of cortical thickness, calculated as the closest distance from the gray/white boundary to the gray/CSF (cerebrospinal fluid) boundary at each vertex on the tessellated surface.[35] The maps were created using spatial intensity gradients across tissue classes and were therefore not simply reliant on absolute signal intensity. The maps produced were not restricted to the voxel resolution of the original data, and thus were capable of detecting sub-millimeter differences between groups. The cortical thickness features were average values for each region. Additionally, for each cortical region, the standard deviation of the cortical thickness was also calculated as a measure of roughness. We should keep in mind that the distribution of cortex thickness is not uniform by layer, neither is the variation in the thickness of the cortical layers proportional to the variation in the total thickness, nor is the location and progression of subtle cortical atrophy the same among individuals with the same

neurodegenerative disease.[8] Hence, there is also a need for new and more reliable variables to analyze the pattern of cortical thickness.[8] "Roughness" within a certain area may therefore be a promising metric to overcome these limitations.[8] An increase in roughness would imply a major cortical thinning (i.e., atrophy).[8]

The above processing steps yielded 129 white matter and grey matter volumetric features of the whole brain (except for the cerebellum) and 152 cortical thickness features (average plus roughness, i.e., standard deviation of the thickness), according to the Desikan-Killiany atlas,[38] resulting in a total of 281 structural features from each subject.

Statistical analyses

Statistical analyses were performed in SPSS Version 23.0 (IBM Corp., NY, USA).

A Student's *t*-test with bootstrapping ($N = 1000$) was applied to MRI data to find significant differences between controls and patients.[39] Equal or unequal variances were considered for the t-tests according to Levene's test results.

To discover relationships between cortical structures and tremor kinematics, all IMUs and hdEMG metrics were linearly modeled by a subset of the 281 structural features extracted from MRI data together with demographic (age and sex) and clinical (Fahn-Tolosa-Marìn tremor rating scale and time from ET onset) variables. For each metric from IMUs or hdEMG, the algorithm built any possible subset of the 281 structural features. For each subset, a Monte Carlo simulation algorithm was applied to find the optimum coefficients of the linear model.[40] Variables were added to the model under a criterion of prevention of overfitting, that is, assessing each new model update on a subset of the total sample. The mean square error of the linear model with respect to the actual values of the target variable was then calculated. Finally, the algorithm returned the model of the subset with the minimum error, thus optimally relating cortical structure to tremor kinematics from an exploratory process. For the current study, only the models of the target variables with an error lower than 20% were reported.

A correlation analysis was also carried out to find the pairwise relationships between hdEMG and IMUs variables, demographic (age and sex), clinical (Fahn-Tolosa-Marìn tremor rating scale and time from ET onset), and structural (MRI) variables. The Pearson product-moment correlation coefficient was calculated for each pair under normality conditions (Shapiro-Wilk test). Spearman's rank correlation coefficient was calculated otherwise. A bootstrapping analysis (1000 samples) was applied to all the correlation calculations to prevent type-I error.[39] The correlations having a significance value of $P < 0.05$ and a confidence interval with lower and upper bounds with the same sign as the correlation value were considered statistically significant.

Results

As this study was nested within the NEUROTREMOR project, a project whose main aim was to technically, functionally and clinically validate a novel system for understanding, providing diagnostic support for, and remotely managing tremors, most of the ET patients who were eligible refused to participate because of lack of time because the study would have required that they come to the hospital several times during the study for the performance of clinical, neurophysiological (magneto-electroencephalography and hdEMG recordings), neuropsychological, and neuroimaging evaluations. Given this constraint, of the 300 ET patients seen at outpatient neurology clinics of the University Hospital "12 de Octubre" in Madrid (Spain) from October 2012 to July 2013, only 47 were eligible for the study. Of these 47 ET patients, 14 had complete neurophysiological testing and an MRI procedure with cortical thickness data. Of these 14 ET patients, one was excluded from the final analyses because he developed incident Parkinson's disease during follow-up. None of the participants were excluded because of neurological comorbidities or structural abnormalities on conventional MRI images, and none or developed additional neurodegenerative diseases during the 5-year-follow-up period.

The final sample of 13 ET patients did not differ to a significant degree from the 17 healthy controls in terms of age, sex, and educational level (Table 2). The mean tremor duration was 27.6 ± 18.7 years and the mean tremor rating scale score was 35.1 ± 13.9 (Table 2).

Linear regression models of hdEMG and IMUs activity from MRI data

Mean logarithmic power of the tremor harmonics, averaged over the AO, PO, and WE tasks, and normalized to RE task (IMU, hand with the more severe tremor)

This linear model was determined by the following equation:

$$y = 0.002 \times \text{left medial orbitofrontal thickness} +$$
$$0.001 \times \text{left supramarginal volume} +$$
$$14.202 \times \text{right isthmus cingulate volume}$$

Thus, the value of the mean logarithmic power of the tremor harmonics, averaged over the AO, PO, and WE

Table 2. Demographic and clinical characteristics of the essential tremor patients and the healthy control group.

	Healthy controls (*N* = 17)	Essential tremor patients (*N* = 13)	*P* value
Sex (men)	10 (58.8%)	6 (46.2%)	$\chi(1) = 0.475$, *P* = 0.491
Age in years	64.1 ± 11.9 (39 to 80)	67.8 ± 7.3 (51 to 80)	$t(28) = -1.008$, *P* = 0.322
Years of formal education	9.1 ± 3.4 (2 to 13)	7.1 ± 3.7 (2 to 12)	$t(26) = 1.491$, *P* = 0.148
Tremor severity [1]	–	35.1 ± 13.9 (18 to 56)	
Tremor duration in years	–	27.6 ± 18.7 (6 to 65)	

Values are expressed as mean ± standard deviation (range).
Student's *t* test was used for comparison of continuous data and the chi-square test for sex proportion.
[1]Fahn–Tolosa–Marín Tremor Rating Scale.

tasks, and normalized to RE task, in the hand with the more severe tremor, was determined by thickness and volume related variables from three cortical areas with a determination coefficient of 0.922, as depicted in Figure 1. Please notice that some of the points in the graph overlap (also in subsequent analogue figures). Figure 1 also shows the relative contribution of the cortical variables to the model. The highest contributions were provided by the supramarginal and medial orbitofrontal areas of the left hemisphere.

Percentage of concurrent motor unit discharges in AO/Percentage of concurrent motor unit discharges in RE (hdEMG in hand with the more severe tremor)

This metric directly measures the synchronization of motor units in AO task, normalized to synchronization of motor units in RE task. Therefore, it reflects the change in motor unit synchronization when the patient moves from the AO to the RE task. This variable was linearly modeled by the following expression:

$$y = -\,2.240 \times \text{right paracentral thickness} -$$
$$2.227 \times \text{left isthmus cingulate thickness}$$

The model comprised two thickness-related variables with different contribution degrees as shown in Figure 2 and adjusted the actual values of the variable with a determination coefficient of 0.813. In this case, the left isthmus of the cingulate gyrus and right paracentral lobule accounted for the total model variance.

Percentage of concurrent motor unit discharges in PO/Percentage of concurrent motor unit discharges in RE (hdEMG in hand with the more severe tremor)

This variable is analogous to the latter one but for the PO task. The model obtained for this variable adjusted

with a coefficient of determination of 0.820. It was defined by the following equation:

$$y = -\,2.687 \times \text{left isthmus cingulate thickness} -$$
$$2.049 \times \text{right paracentral thickness}$$

The cortical areas accounting for the model variance are the same as for the AO task, as shown in Figure 3. However, in this case the contribution of the left isthmus of the cingulate gyrus is higher than the right paracentral lobule.

Percentage of concurrent motor unit discharges in AO/Percentage of concurrent motor unit discharges in RE (hdEMG in hand with the less severe tremor)

$$y = -\,16.800 \times \text{right paracentral roughness} - 11.009 \times$$
$$\text{right lingual roughness} + 565.029 \times$$
$$\text{left thalamus proper volume/grey matter volume} -$$
$$2641.681 \times \text{left amygdala volume/intracraneal volume}$$

The value of this variable was determined by the following linear model:

In this case, the model was defined by two roughness-related cortical variables in the right hemisphere, with the same highest contribution, and two volume-related subcortical variables (Fig. 4). The determination coefficient of this model was 0.979.

MRI differences between ET patients and healthy controls

Table 3 lists the brain anatomical areas that showed significant differences between ET patients and the healthy control group. Differences (reduced volume, lower thickness and higher roughness) localized to certain subcortical and cortical regions, which included both thalami, left sensorimotor cortex, left temporal lobe, left occipital areas, left cingulate areas and
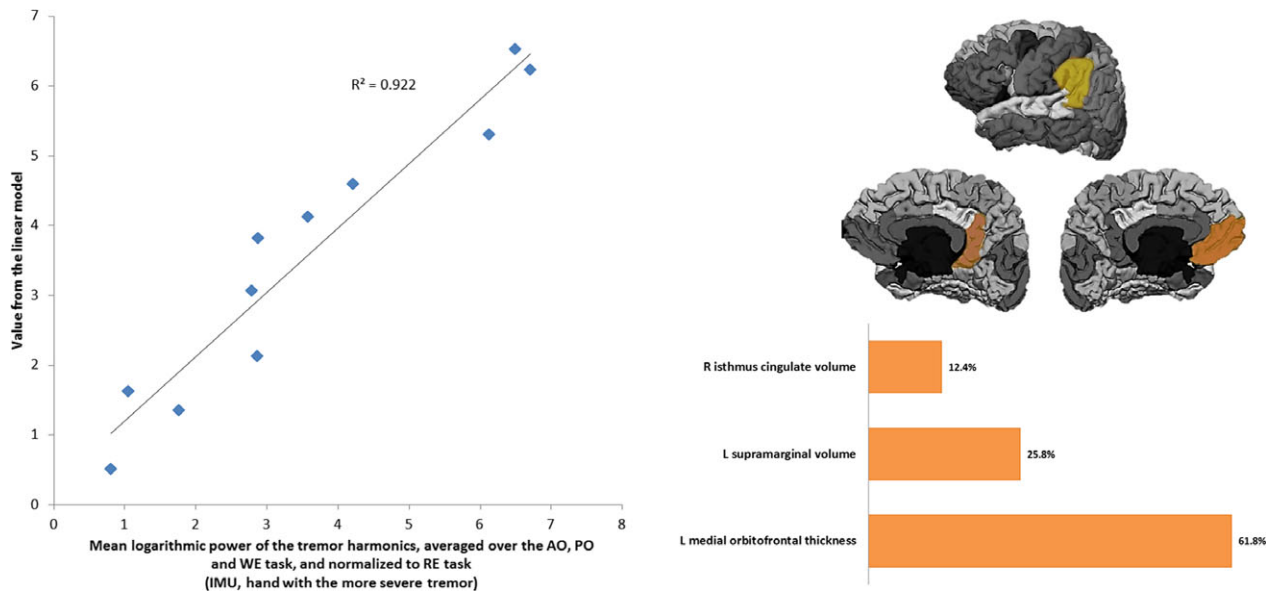
Figure 1. Left: Linearly modeled versus actual values of the mean logarithmic power of the tremor harmonics averaged over the AO, PO and WE tasks, and normalized to RE task in the hand with the more severe tremor. Right: Cortical areas comprising the descriptive model and their relative contribution. L: Left hemisphere; R: Right hemisphere.

Figure 2. Left: Linearly modeled versus actual values of the percentage of concurrent motor unit discharges in AO task normalized to RE in the hand with the more severe tremor. Right: Cortical areas comprising the descriptive model and their relative contribution. L: Left hemisphere; R: Right hemisphere.

bilateral entorhinal and ventral areas. Of note is that none of these areas, aside from the left thalamus, were part of the linear models described above, which suggests a dissociation between the areas associated with the diagnosis and the ones modulating (or modulated) by the severity of tremor.

Correlations between IMUs and hdEMG metrics and MRI, demographic and clinical features

Table 4 shows the statistically significant correlations between IMUs and hdEMG metrics and MRI data,

Figure 3. Left: Linearly modeled versus actual values of the percentage of concurrent motor unit discharges in PO task normalized to RE in the hand with the more severe tremor. Right: Cortical areas comprising the descriptive model and their relative contribution. L: Left hemisphere; R: Right hemisphere.
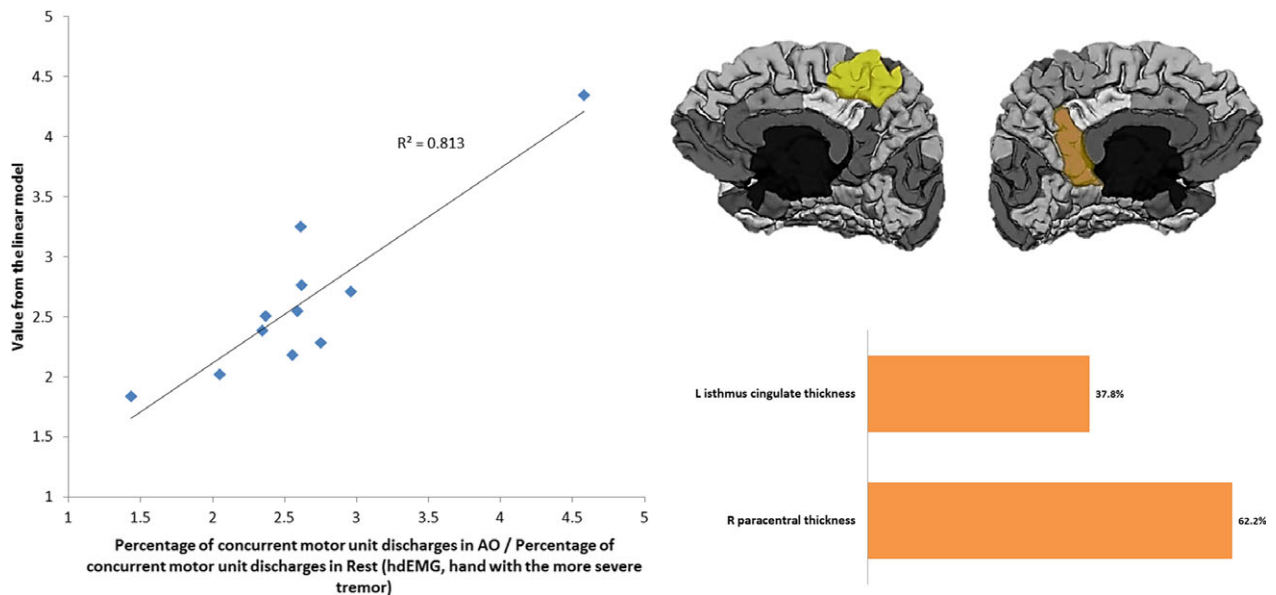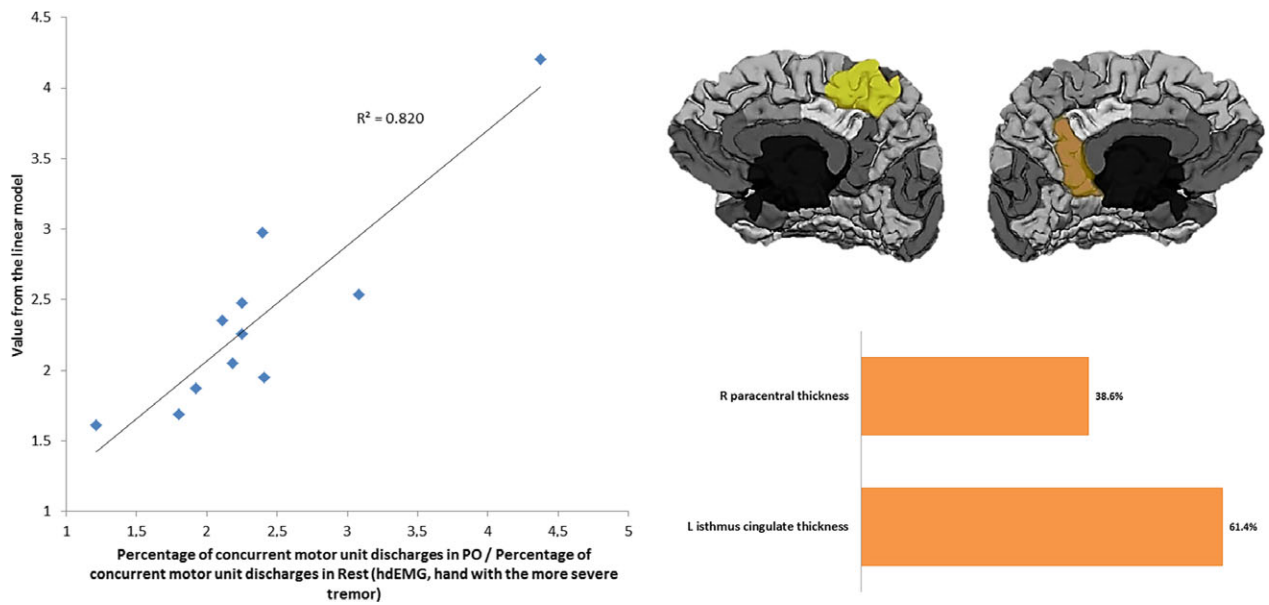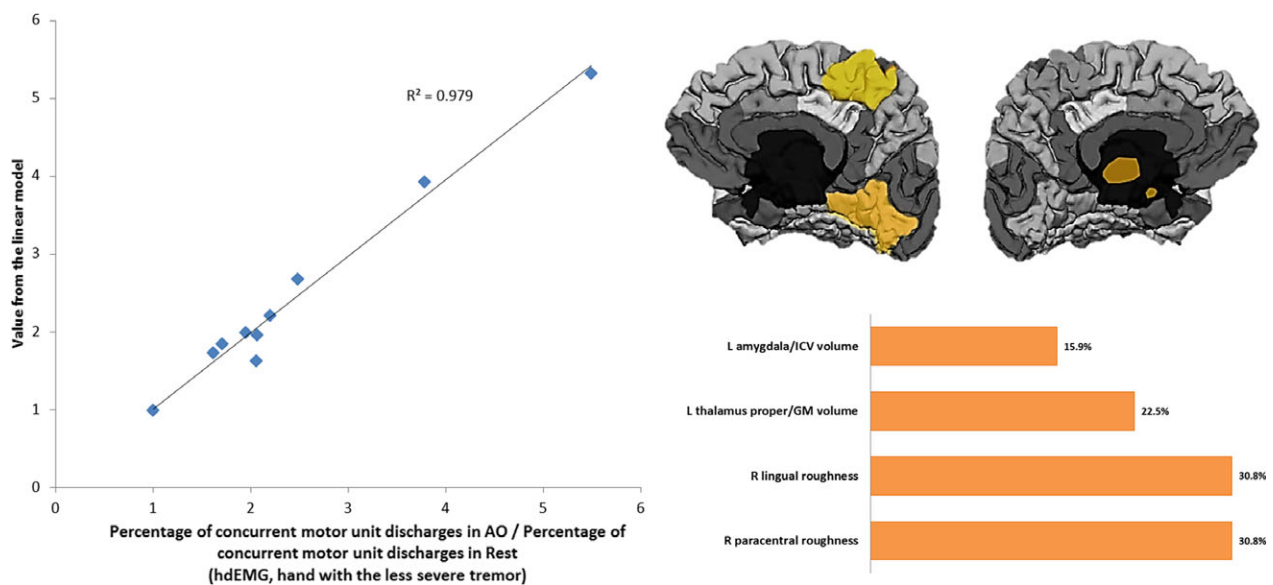

Figure 4. Left: Linearly modeled versus actual values of the percentage of concurrent motor unit discharges in AO task normalized to RE in the hand with the less severe tremor. Right: Cortical areas comprising the descriptive model and their relative contribution. L: Left hemisphere; R: Right hemisphere; GM: Grey Matter; ICV: Intracraneal Volume.

demographic and clinical features. Only two of the IMUs or hdEMG metrics, which were linearly modeled above, presented significant correlations with the MRI data conforming their respective linear models (Table 4). In addition, several MRI variables in the linear models above showed significant correlations with different IMUs/

hdEMG variables, such as the left isthmus of the cingulate gyrus thickness and the right paracentral lobule roughness, pointing to a relationship between all these variables and tremor parameters. With respect to clinical variables, the Fahn-Tolosa-Marín tremor rating scale score was positively correlated with sex (women tended to a higher

Table 3. Statistically significant differences (*t*-test, *P < 0.05*) of MRI morphometry features between the essential tremor patients and the healthy control group.

| | Healthy controls (N = 17) | Essential tremor patients (N = 13) | P value | Bootstrapping (N=1000) | |
| | | | | Confidence Interval | |
				Lower	Upper
Left thalamus proper volume	6157 ± 903	5530 ± 498	0.004	260.046	1472.456
Right thalamus proper volume	6053 ± 656	5507 ± 730	0.011	170.462	1179.054
Right thalamus proper volume/ intracranial volume	0.0037 ± 0.0004	0.0034 ± 0.0004	0.047	0.0000076	0.0009711
Left superior parietal volume	12725 ± 1588	11363 ± 1181	0.005	528.311	2614.395
Left precuneus volume	8824 ± 1088	7786 ± 1060	0.005	327.191	1668.239
Left entorhinal volume	1997 ± 269	1630 ± 420	0.006	130.273	711.229
Left precentral thickness	2.5362 ± 0.1114	2.4441 ± 0.1314	0.025	0.01425	0.20172
Left postcentral thickness	2.1361 ± 0.1214	2.0444 ± 0.1073	0.009	0.03168	0.20129
Left temporal lobe thickness	2.9566 ± 0.1489	2.8277 ± 0.1643	0.016	0.02660	0.23891
Left parahippocampal thickness	2.8657 ± 0.3863	2.3518 ± 0.7359	0.035	0.02208	0.56041
Left posterior temporal roughness	0.4662 ± 0.0615	0.5164 ± 0.0747	0.024	−0.11178	-0.00856
Right lateral orbitofrontal volume	7190 ± 853	6592 ± 701	0.014	170.850	1383.304
Right fusiform volume	9270 ± 1314	8247 ± 1283	0.007	392.988	2312.406
Right entorhinal volume	1709 ± 304	1451 ± 265	0.008	76.055	473.366

Values are expressed as mean ± standard deviation.

score) and the left medial orbitofrontal cortex roughness. This latter variable was a significant part of the linear model of the mean logarithmic power of the tremor harmonics, averaged over the AO, PO, and WE tasks, and normalized to RE task, in the hand with the more severe tremor. The time from onset variable was positively correlated with age, and negatively correlated with the left amygdala volume with respect to the intracranial volume. Finally, age was negatively correlated with the left isthmus of the cingulate gyrus thickness, which is in turn part of the linear model of the percentage of concurrent motor unit discharges in AO normalized to RE in the hand with the more severe tremor.

Discussion

We have demonstrated for the first time that morphological changes in fronto-parietal circuit areas that regulate movement sequencing are associated with increased motor unit synchronization in the wrist muscles and, consequently, with severity of tremor in ET patients. Noteworthy, similar results were suggested for Parkinson's disease.[10] Increased motor unit synchronization (i.e., more severe tremor) was associated with cortical changes (i.e., atrophy) in widespread cortical areas, including the left medial orbitofrontal cortex, left isthmus of the cingulate gyrus, right paracentral lobule, right lingual gyrus, as well as reduced left supramarginal gyrus (left inferior parietal cortex), right isthmus of the cingulate gyrus, left thalamus, and left amygdala volumes. The

majority of these brain anatomical areas are involved in controlling movement sequencing.[41] The fact that multiple cortical changes were affected at the same time suggests the presence of a widespread functional network involvement associated with tremor severity in ET patients. In other words, these data suggest that the propogation and features of ET may be impacted by multiple nodes along a cerebellar-thalamic-cortical network.[42]

All of our ET patients had bilateral tremor. We have demonstrated that a large degree of tremor symmetry exists in the neural drive to extensors and flexors of the right and left wrist.[15] This at least partially explains why the cortical changes found in both hemispheres were statistically connected to the tremor demonstration in the hand with more tremor. Further analysis of the interactions between the bilateral cortical changes and bilateral tremor demonstration are required.

Frontal and parietal areas are essential in attending to and/or modeling motor action.[41] Furthermore, left parietal cortex damage or transcranial magnetic stimulation of the left parietal cortex causes problems in performing movement sequences.[43,44] The posterior parietal cortex, including the inferior parietal lobule, has been shown to be involved in the preparation and redirection of movements.[45] as well as in intention to perform specific motor acts.[46] Also, the parietal cortex has interactions with the extrastriate body area.[47] This area, which is located in the lateral occipital cortex at the posterior end of the inferior temporal sulcus, is well-known to respond to visual processing of static and moving human bodies even in the

Table 4. Matrix of statistically significant correlations ($P < 0.05$, bilateral) between IMUs and hdEMG metrics and MRI data, demographic and clinical features.

Bootstrapping (N=1000)		Age	FTM	Time from tremor onset	Mean logarithmic power of the tremor harmonics averaged over the AO, PO and WE tasks and normalized to RE task (IMU in hand with the more severe tremor)	Percentage of concurrent motor unit discharges in AO/Percentage of concurrent motor unit discharges in RE (hdEMG in hand with the more severe tremor)	Percentage of concurrent motor unit discharges in PO/Percentage of concurrent motor unit discharges in RE (hdEMG in hand with the more severe tremor)
Age in years	Coefficient			0.790[1]			
	P value			0.011			
Sex	Coefficient		0.783[2]				
	P value		0.013				
Left Amygdala volume/ICV	Coefficient			−0.688[1]			
	P value			0.40			
Left supramarginal volume	Coefficient				0.704[1]		
	P value				0.034		
Left isthmus cingulate thickness	Coefficient	−0.739[1]			−0.754[1]		
	P value	0.023			0.19		
Left medial orbitofrontal roughness	Coefficient		0.778[2]				
	P value		0.014				
Right isthmus cingulate volume	Coefficient				0.717[2]		
	P value				0.030		
Right paracentral roughness	Coefficient					−0.723[2]	−0.714[2]
	P value					0.028	0.021

[1]Pearson product-moment correlation coefficient.
[2]Spearman's rank correlation coefficient.
Arms outstretched (AO); arms supported + postural tremor elicited (PO); arms outstretched with weights (WE); rest (RE); Fahn Tolosa-Marín tremor rating scale (FTM); high-density surface electromyography (hdEMG); inertial measurement unit (IMU); intracraneal volume (ICV).

absence of visual feedback from the limb.[48] In addition, the extrastriate body area contributes to planning goal-directed actions, possibly by specifying a desired postural configuration to parieto-frontal areas involved in computing movement parameters.[47] We also found thinning of the right lingual gyrus, suggesting dysfunction of the visual associative cortex. This finding supports previous neuropsychological studies of ET patients that suggest impaired visual-motor integration,[49] and structural brain changes in these areas.[50] Visual-associative cortical areas (i.e., lingual gyrus) damage (atrophy) may impair processing of somatosensory and visual stimuli, crucial for correct spatial and temporal motor control.

Notably, we found that the paracentral lobule was affected. The anterior portion of the paracentral lobule is part of the frontal lobe and is often referred to as the supplementary motor area.[51] It is recognized that the supplementary motor area plays a role in the planning, initiation, and execution of motor acts. Furthermore, there is a positive correlation between supplementary motor area activity and the ordinal complexity of a sequence of movements.[52]

Of additional interest, we found that the left medial orbitofrontal cortex and the left amygdala were affected. The medial orbitofrontal cortex is part of a neural substrate that allows for the explicit retrieval of cognitive strategies and of learned motor routines involved during the skilled performance of sequential movement.,[53] meanwhile the amygdala is a key brain area regulating many aspects of emotional processing, including recognition of emotional expression in faces. Both brain areas could be affected in ET patients.[54,55] Specifically, facial emotion recognition has been found inversely correlated with tremor severity (i.e., the lower facial emotion recognition, the more severe tremor intensity).[55]

Another key finding of our study is that cingulate cortex changes bilaterally were associated with increased motor unit synchronization and, therefore, more tremor

severity. The cingulate cortex may also be involved in some way with the modulation of movement sequencing since the anterior cingulate cortex plays a key role in relating actions to their consequences, both positive reinforcement outcomes and errors, and in guiding decisions about which actions are worth making.[56]

Taken together, the cortical changes observed in these regions may indicate that ET patients might be more inefficient in integrating multi-modal information in the fronto-parietal network to produce an output that reflects the selection, preparation, and execution of movements,[57] which would result in tremor generation.

The observed cortical thickness changes may be caused by sustained neuronal activation and subsequent neuronal damage or loss. Alternative explanations include changes in energy demand of sensory and motor neural loops.[58] Indeed, increased motor unit synchronization has been demonstrated to correlate with higher central and peripheral muscle fatigue.[59] Therefore, higher energy demand could facilitate neuronal damage with subsequent cortical thinning (i.e., atrophy). An alternative explanation is that the changes we observed are due to neurodegeneration. A recent study has shown that volume loss is not restricted solely to the cerebellum in ET, and that gray matter volume loss appears to be widespread in the cerebrum as well.[60] Similarly, studies of patients with diseases characterized by even greater cerebellar involvement than in ET (e.g., spinocerebellar ataxias) indicate the presence of volume loss in the cerebral cortex as well, indicating a more diffuse degeneration in those diseases.[61,62]

It is worth mentioning that different variables of different nature (IMUs, hdEMG or clinical features) were correlated with different anatomical regions and features of the cortical anatomy. This is likely because they are measuring different phenomena, despite all being related to tremor severity. Tremor severity depends on the strength of pathological muscle excitation. This strength will dictate both the number of recruited motor units as well as their synchronization. Whereas the percentage of concurrent motor unit discharges measures the strength of pathological excitation in each individual muscle, the IMUs-based metrics introduced herein measure the net effect of the excitation of all the muscles controlling the wrist. In addition, the phase differences (i.e., timing) in excitation of different muscles have been demonstrated to have a significant effect on amplitude of wrist movement and, therefore, IMUs-based metrics.[17] These differences in sensitivity of IMUs-based and hdEMG –based metrics used in this study could at least partially explain the correlation with different anatomical regions and features of the cortex.

Several limitations of our study need to be mentioned. First, the sample size was relatively small. However, we observed robust correlations. Notwithstanding, it would be important to replicate these findings in a larger sample, as small samples may be subject to spurious findings. Second, the diagnosis of ET was based on clinical criteria and further supported by normal [(123) I]FP-CIT single photon emission computed tomography scan results. Finally, it was not possible to determine whether there were abnormalities in the cerebellum. Numerous clinical, neuroimaging, and postmortem studies indicate the presence of functional, metabolic, and structural abnormalities in the cerebellum of ET patients.[63] In the current study, cortical reconstruction and volumetric segmentation was performed with the FreeSurfer image analysis suite (http://surfer.nmr.mgh.harvard.edu/). It is currently not possible to obtain cortical thickness from cerebellum with FreeSurfer, since this structure has such a fine cortex that you need resolution on the order of microns to actually get it properly (http://surfer.nmr.mgh.harvard.edu/).

In closing, given that the accurate control of movement sequencing is important for motor behavior programs and that the responsible brain areas mainly overlap with those involved in controlling motor sequencing, our results suggest that ET tremor may be the result of an involuntary activation of a program of motor behavior ordinarily used in the genesis of rapid voluntary alternating movements. These brain anatomical areas could conceivably represent new targets for neurostimulation approaches, such as repetitive transcranial magnetic stimulation or transcranial current direct stimulation, to provide new approaches to long-lasting reduction in tremor.

Acknowledgments

Author Contribution

Dr. Benito-León collaborated in: (1) the conception, organization of the research project; (2) the statistical analysis design, and (3) the writing of the manuscript first draft and the review and critique of the manuscript. Dr. Serrano collaborated in: (1) the conception, organization and execution of the research project; (2) the statistical analysis design, and; (3) and the review and critique of the manuscript. Dr. Louis collaborated in: (1) the conception, organization of the research project; and (2) the review and critique of the manuscript. Dr. Holobar collaborated in: (1) the conception, organization of the research project; and (2) the review and critique of the manuscript. Dr. Romero collaborated in: (1) the conception, organization of the research project; and (2) the review and critique of the manuscript. Dr. Povalej-Bržan collaborated in: (1) the conception, organization of the

research project; and (2) the review and critique of the manuscript. Mr. Kranjec collaborated in: (1) the conception, organization of the research project; and (2) the review and critique of the manuscript. Dr. Bermejo-Pareja collaborated in: (1) the conception, organization of the research project; and 2) the review and critique of the manuscript. Dr. del Castillo collaborated in: (1) the conception, organization of the research project; (2) the statistical analysis design; and (3) the review and critique of the manuscript. Dr. Posada collaborated in: (1) the conception, organization of the research project; and 2) the review and critique of the manuscript. Dr. Rocon collaborated in: (1) the conception, organization of the research project; and (2) the review and critique of the manuscript.

Conflict of Interest

The authors declare no competing financial interests.

References

1. Benito-León J. Essential tremor: a neurodegenerative disease? Tremor Other Hyperkinet Mov (N Y) 2014;4:252.

2. Raethjen J, Govindan RB, Kopper F, et al. Cortical involvement in the generation of essential tremor. J Neurophysiol 2007;97:3219–3228.

3. Ibanez J, González de la Aleja J, Gallego JA, et al. Effects of alprazolam on cortical activity and tremors in patients with essential tremor. PLoS ONE 2014; 9:e93159.

4. Sharifi S, Luft F, Verhagen R, et al. Intermittent cortical involvement in the preservation of tremor in essential tremor. J Neurophysiol 2017;118:2628–2635. jn 00848 2016.

5. Archer DB, Coombes SA, Chu WT, et al. A widespread visually-sensitive functional network relates to symptoms in essential tremor. Brain 2017;141:472–485.

6. Chung SJ, Kwon H, Lee DK, et al. Neuroanatomical heterogeneity of essential tremor according to propranolol response. PLoS ONE 2013;8:e84054.

7. Cerasa A, Nistico R, Salsone M, et al. Neuroanatomical correlates of dystonic tremor: a cross-sectional study. Parkinsonism Relat Disord 2014;20:314–317.

8. Serrano JI, Romero JP, Castillo MDD, et al. A data mining approach using cortical thickness for diagnosis and characterization of essential tremor. Sci Rep 2017;7:2190.

9. Benito-León J, Louis ED, Bermejo-Pareja F, Neurological Disorders in Central Spain Study G. Risk of incident Parkinson's disease and parkinsonism in essential tremor: a population based study. J Neurol Neurosurg Psychiatry 2009;80:423–425.

10. Benito-León J, Serrano JI, Louis ED, et al. Tremor severity in Parkinson's disease and cortical changes of areas

11. Gallego JA, Dideriksen JL, Holobar A, et al. Influence of common synaptic input to motor neurons on the neural drive to muscle in essential tremor. J Neurophysiol 2015;113:182–191.

12. American Psychiatric A. Diagnostic and Statistical Manual of Mental Disorders DSM-IV. Washington 1994.

13. Fahn S, Tolosa E, Conceppcion M. Clinical rating scale for tremor. In: Jankovic J, Tolosa E, eds. Parkinson's Disease and Movement Disorders. Baltimore, MD: Williams and Wilkins, 1993:271–280.

14. Deuschl G, Bain P, Brin M. Consensus statement of the movement disorder society on tremor. Ad hoc scientific committee. Mov Disord. 1998;13(Suppl 3):2–23.

15. Povalej Brzan P, Gallego JA, Romero JP, et al. New perspectives for computer-aided discrimination of parkinson's disease and essential tremor. Complexity 2017;2017:1–17.

16. Dideriksen JL, Gallego JA, Holobar A, et al. One central oscillatory drive is compatible with experimental motor unit behaviour in essential and Parkinsonian tremor. J Neural Eng 2015;12:046019.

17. Gallego JA, Dideriksen JL, Holobar A, et al. The phase difference between neural drives to antagonist muscles in essential tremor is associated with the relative strength of supraspinal and afferent input. J Neurosci 2015;35:8925–8937.

18. Negro F, Farina D. Linear transmission of cortical oscillations to the neural drive to muscles is mediated by common projections to populations of motor neurons in humans. J Physiol 2011;589:629–637.

19. Farina D, Negro F, Jiang N. Identification of common synaptic inputs to motor neurons from the rectified electromyogram. J Physiol 2013;591:2403–2418.

20. Farina D, Merletti R, Enoka RM. The extraction of neural strategies from the surface EMG: an update. J Appl Physiol (1985). 2014;117:1215–1230.

21. Pfander GE, Walnut DF. Sampling and reconstruction of operators. IEEE Trans Inf Theory 2016;62:435–458.

22. Hartman WM. Signals, Sound, and Sensation. p.109. Berlin, Germany: Springer Science & Business Media, 2004.

23. Muthuraman M, Heute U, Arning K, et al. Oscillating central motor networks in pathological tremors and voluntary movements. What makes the difference? NeuroImage 2012;60(2):1331–1339.

24. Muthuraman M, Hossen A, Heute U, et al. A new diagnostic test to distinguish tremulous Parkinson's disease from advanced essential tremor. Mov Disord 2011;26:1548–1552.

25. Holobar A, Farina D, Gazzoni M, et al. Estimating motor unit discharge patterns from high-density surface electromyogram. Clin Neurophysiol 2009;120:551–562.

26. Holobar A, Glaser V, Gallego JA, et al. Non-invasive characterization of motor unit behaviour in pathological tremor. J Neural Eng 2012;9:056011.

27. Holobar A, Minetto MA, Farina D. Accurate identification of motor unit discharge patterns from high-density surface EMG and validation with a novel signal-based performance metric. J Neural Eng 2014;11:016008.

28. De Luca CJ, Roy AM, Erim Z. Synchronization of motor-unit firings in several human muscles. J Neurophysiol 1993;70:2010–2023.

29. Glaser V, Farina D, Holobar A. Simulations of high-density surface electromyograms in dynamic muscle contractions. Conf Proc IEEE Eng Med Biol Soc 2017;2017:3453–3456.

30. Reuter M, Rosas HD, Fischl B. Highly accurate inverse consistent registration: a robust approach. NeuroImage 2010;53:1181–1196.

31. Segonne F, Dale AM, Busa E, et al. A hybrid approach to the skull stripping problem in MRI. NeuroImage 2004;22:1060–1075.

32. Fischl B, Salat DH, van der Kouwe AJ, et al. Sequence-independent segmentation of magnetic resonance images. NeuroImage 2004;23(Suppl 1):S69–S84.

33. Sled JG, Zijdenbos AP, Evans AC. A nonparametric method for automatic correction of intensity nonuniformity in MRI data. IEEE Trans Med Imaging 1998;17:87–97.

34. Segonne F, Pacheco J, Fischl B. Geometrically accurate topology-correction of cortical surfaces using nonseparating loops. IEEE Trans Med Imaging 2007;26:518–529.

35. Fischl B, Dale AM. Measuring the thickness of the human cerebral cortex from magnetic resonance images. Proc Natl Acad Sci U S A. 2000;97:11050–11055.

36. Fischl B, Sereno MI, Dale AM. Cortical surface-based analysis. II: Inflation, flattening, and a surface-based coordinate system. NeuroImage 1999;9:195–207.

37. Dale AM, Fischl B, Sereno MI. Cortical surface-based analysis. I. Segmentation and surface reconstruction. Neuroimage 1999;9:179–194.

38. Desikan RS, Segonne F, Fischl B, et al. An automated labeling system for subdividing the human cerebral cortex on MRI scans into gyral based regions of interest. NeuroImage 2006;31:968–980.

39. Henderson AR. The bootstrap: a technique for data-driven statistics. Using computer-intensive analyses to explore experimental data. Clin Chim Acta 2005;359:1–26.

40. Lamnisos D, Griffin JE, Steel MFJ. Adaptive monte carlo for bayesian variable selection in regression models. J Comput Grap Stat 2013;22:729–748.

41. Bengtsson SL, Ehrsson HH, Forssberg H, Ullen F. Dissociating brain regions controlling the temporal and ordinal structure of learned movement sequences. Eur J Neurosci 2004;19:2591–2602.

42. Hallett M. Tremor: pathophysiology. Parkinsonism Relat Disord 2014;20(Suppl 1):S118–S122.

43. Rushworth MF, Nixon PD, Renowden S, et al. The left parietal cortex and motor attention. Neuropsychologia 1997;35:1261–1273.

44. Rushworth MF, Ellison A, Walsh V. Complementary localization and lateralization of orienting and motor attention. Nat Neurosci 2001;4:656–661.

45. Rushworth MF, Johansen-Berg H, Gobel SM, Devlin JT. The left parietal and premotor cortices: motor attention and selection. NeuroImage 2003;20(Suppl 1):S89–S100.

46. Desmurget M, Reilly KT, Richard N, et al. Movement intention after parietal cortex stimulation in humans. Science 2009;324:811–813.

47. Zimmermann M, Mars RB, de Lange FP, et al. Is the extrastriate body area part of the dorsal visuomotor stream? Brain Struct Funct 2018;223:31–46.

48. Lingnau A, Downing PE. The lateral occipitotemporal cortex in action. Trends Cogn Sci 2015;19:268–277.

49. Bares M, Lungu OV, Husarova I, Gescheidt T. Predictive motor timing performance dissociates between early diseases of the cerebellum and Parkinson's disease. Cerebellum 2010;9:124–135.

50. Benito-León J, Álvarez-Linera J, Hernández-Tamames JA, et al. Brain structural changes in essential tremor: voxel-based morphometry at 3-Tesla. J Neurol Sci 2009;287:138–142.

51. Conn PM. Neuroscience in medicine, 2nd ed. Totowa, N.J.: Humana Press, 2003.

52. Boecker H, Dagher A, Ceballos-Baumann AO, et al. Role of the human rostral supplementary motor area and the basal ganglia in motor sequence control: investigations with H2 15O PET. J Neurophysiol 1998;79:1070–1080.

53. Lafleur MF, Jackson PL, Malouin F, et al. Motor learning produces parallel dynamic functional changes during the execution and imagination of sequential foot movements. NeuroImage 2002;16:142–157.

54. Chatterjee A, Jurewicz EC, Applegate LM, Louis ED. Personality in essential tremor: further evidence of non-motor manifestations of the disease. J Neurol Neurosurg Psychiatry 2004;75:958–961.

55. Auzou N, Foubert-Samier A, Dupouy S, Meissner WG. Facial emotion recognition is inversely correlated with tremor severity in essential tremor. J Neural Transm (Vienna) 2014;121:347–351.

56. Rushworth MF, Walton ME, Kennerley SW, Bannerman DM. Action sets and decisions in the medial frontal cortex. Trends Cogn Sci 2004;8:410–417.

57. Wise SP, Boussaoud D, Johnson PB, Caminiti R. Premotor and parietal cortex: corticocortical connectivity and combinatorial computations. Annu Rev Neurosci 1997;20:25–42.

58. Mangia S, Tkac I, Gruetter R, et al. Sustained neuronal activation raises oxidative metabolism to a new steady-

state level: evidence from 1H NMR spectroscopy in the human visual cortex. J Cereb Blood Flow Metab 2007;27:1055–1063.

59. Boyas S, Guevel A. Neuromuscular fatigue in healthy muscle: underlying factors and adaptation mechanisms. Ann Phys Rehabil Med 2011;54:88–108.

60. Cameron E, Dyke JP, Hernández N, et al. Cerebral gray matter volume losses in essential tremor: a case-control study using high resolution tissue probability maps. Parkinsonism Relat Disord 2018;51:85–90.

61. Dohlinger S, Hauser TK, Borkert J, et al. Magnetic resonance imaging in spinocerebellar ataxias. Cerebellum 2008;7:204–214.

62. Hernández-Castillo CR, Gálvez V, Díaz R, Fernández-Ruiz J. Specific cerebellar and cortical degeneration correlates with ataxia severity in spinocerebellar ataxia type 7. Brain Imaging Behav 2016;10:252–257.

63. Louis ED. Essential tremor and the cerebellum. Handb Clin Neurol 2018;155:245–258.